JOC The Journal of Organic Chemistry

pubs.acs.org/joc Note

C−F Bonds as "Frozen" Nucleophiles: Unconsummated S_N2 Reactions

Stefan Andrew Harry, Nathaniel G. Garrison, Andrea Zhu, Michael Richard Xiang, Maxime A. Siegler, and Thomas Lectka*

Cite This: J. Org. Chem. 2022, 87, 13406−13410 Read Online

ACCESS | Metrics & More | Article Recommendations | Supporting Information

ABSTRACT: In this note, we present a series of rigid molecules that show close enforced interactions between Ar−F moieties and $-CH_2X$ groups in a "tetrel bond" configuration similar to a nascent S_N2 attack. We explore the spectroscopic, crystallographic, and chemical reactivity consequences of these unusual interactions, including significant through-space spin−spin couplings, short C−F···CH_2X distances, and differential S_N1 and S_N2 reaction pathways. We also reveal experimental evidence of carbon-based tetrel bonds influencing chemical reactivity in solution. Finally, density functional theory (DFT) calculations are employed throughout this study to confirm and illuminate our experimental data.

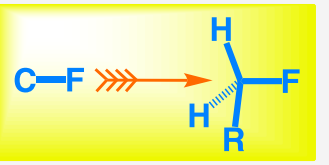

Modern studies on the nature of C−F bonds in medicinal chemistry have revealed a wealth of different roles they can play aside from their traditional role as torpid entities that deactivate molecules toward reactivity and degradation.[1] As such, we are intrigued by the view of fluorine in a C−F bond as an interrupted or "frozen" nucleophile unlikely to engage in covalent bond formation, which stands in contrast to other heteroatoms containing lone pairs of electrons, such as −SH, −OH, or $-NH_2$ (Figure 1). This "snapshot in place" could

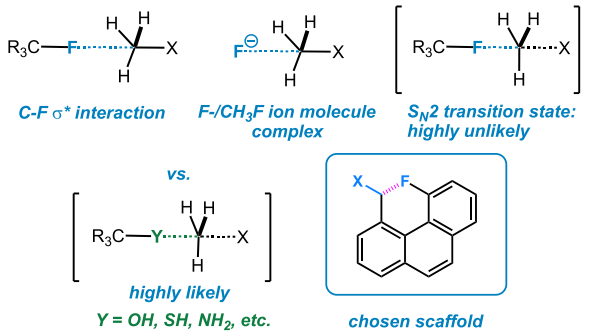

Figure 1. Frozen C−F···C—X interactions.

provide valuable insights into fluorine's role in macromolecular stabilization without presenting a danger of unwanted reactivity.[2] In this note, we present a study of a series of molecules showing close interactions between Ar−F moieties and $-CH_2X$ groups in a configuration similar to a nascent S_N2[3] attack in an ion−molecule complex.[4] We also explore the spectroscopic and chemical reactivity consequences of these interesting C−F σ^*-arrangements.

This so-called "σ-hole" interaction was recently proposed by Arurun et al.[5] and eventually characterized as a "tetrel bond" after it was discovered that Si, Ge, and Sn exhibit similar behavior.[6] While there is significant computational support for tetrel bonding in organic species, the weak and transient nature of tetrel bonds have limited experimental evidence to either crystallographic surveys[7] or higher-order members of group 14 in the periodic table.[8,9] Our present experimental study also complements the computational report by Grabowski and co-workers that predicted that tetrel bonding interactions often precede S_N2 reactions between more traditional Lewis bases and group 14 atoms.[10]

We chose a 4,5-disubstituted phenanthrene core[11] as an optimal scaffold to illustrate the problem (Figure 1).[12] A disubstituted "bay" region forces the protonucleophile and the electrophile to be within striking distance of one another. The synthesis began with a Wittig reaction of 3,5-xylylmethyl-triphenylphosphonium bromide[13] and 3,5-difluorobenzaldehyde (Li metal and MeOH). Mallory cyclization (I_2 at 254 nm)[14] affords the basic core and control (**1-H**) that could then be functionalized further. Radical dibromination of **1-H** affords **1-Br** (66% yield), and treatment with TBAF/*t*-BuOH[15] elaborates **1-Br** to **1-F**. Silver-promoted sequential hydrolysis/oxidation of **1-Br**, followed by catalytic hydrogenation, gives **1-OH**, which upon dichlorination ($SOCl_2$ and CH_2Cl_2) yields **1-Cl**. Thus, a homologous series (H, F, Cl, and Br) was made available for comparison (Figure 2).

To begin, NMR studies of the probe molecules (**1-F**, **1-Cl**, and **1-Br**) revealed some interesting trends (Figure 3). A prominent $^{19}F-^{13}C$ through-space coupling of 41.5 Hz in **1-F**

Received: July 27, 2022
Published: September 27, 2022

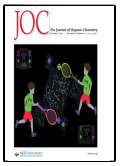

https://doi.org/10.1021/acs.joc.2c01788
J. Org. Chem. 2022, 87, 13406−13410

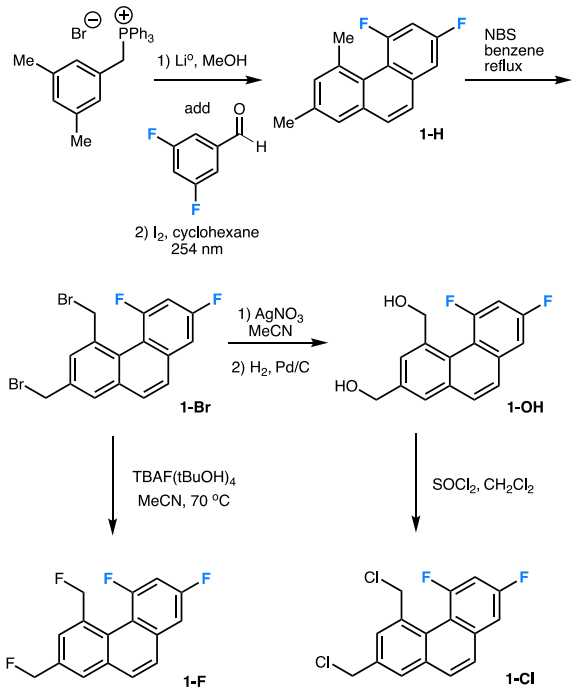

Figure 2. Synthesis of candidates **1-H**, **1-Br**, **1-OH**, **1-F**, and **1-Cl**.

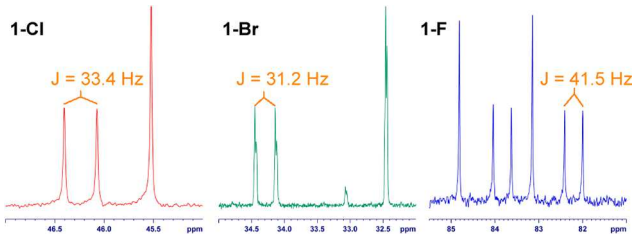

Figure 3. $^{19}F-^{13}C$ through-space coupling for halogenated compounds.

(400 MHz, $CDCl_3$) indicates a strong interaction between Ar–*F* and $-CH_2X$.[16] Of course, analogous through-space couplings are well-known, although our example presents an uncommonly large magnitude.[17]

This coupling decreases somewhat in **1-Cl** (33.4 Hz) and **1-Br** (31.2 Hz). These values align well with the density functional theory (DFT) calculated trends "M06" (M06-2*X*/6-311++G**).[18] If the assumption is that spin information is primarily transferred through an n → σ^* interaction, the empirical and computational ordering makes sense, as the best energy match exists between the low-lying σ^*(C–F) and a lone pair on Ar–F.[19] This prediction is mirrored in the isodesmic relations shown in Figure 4, where the interaction contributes to the stabilization of the system by −3.6 kcal/mol for Br, −1.9 kcal for Cl, and −1.1 kcal for H (M06).[20] NBO analysis further supports this prediction, as the σ^*(C–F) of the probe $-CH_2F$ group of **1-F** predicts 41% higher occupancy than σ^*(C–F) of the control group. In contrast, the probe positions of **1-Cl** and **1-Br** show 28% and 25% decreases in occupancy, respectively, with respect to control groups, whereas **1-H** reveals no difference. Additionally, the measured $^{19}F-^{13}C$ coupling of 41.5 Hz is strikingly close to a calculated though-space coupling of 39.5–53.1 Hz at a distance of 2.5–2.6 Å in an HF···CH_4 system featuring orbital overlap with a carbon-centered σ^*-orbital.[21]

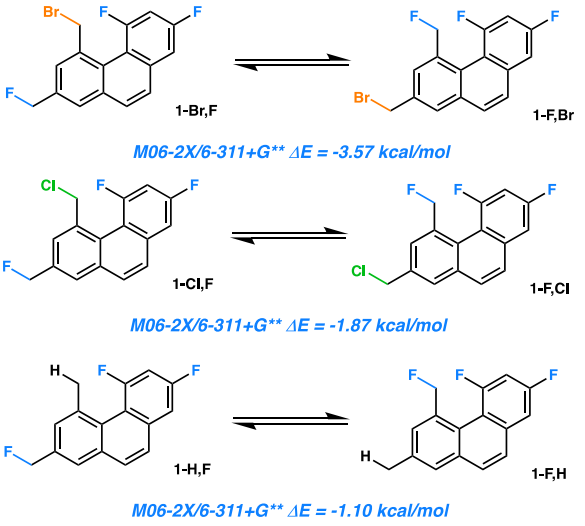

Figure 4. Isodesmic estimations of stabilization energies.

The corresponding through-space J_{HF} couplings between Ar–*F* and $-CH_2X$ (F, Cl, Br) are 7.0, 6.1, and 5.3 Hz, which are also mirrored by the calculation. Curiously, the coupling (*J*) between Ar-*F* and $-CH_2F$ is predicted to be only about 1 Hz. In rotamer **1-F′**, on the other hand, the coupling is projected to soar to 21 Hz as a result of the spatial proximity between the aryl and benzylic fluorine atoms (Figure 5). In the event, we observe no coupling between these two atoms within spectrometric resolution, consistent with the predominance of rotamer **1-F** in solution.

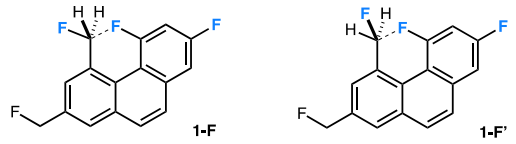

Figure 5. Rotameric forms of **1-F**.

Electrostatic potential surface maps illuminate other features and trends (M06, calcd. using the Spartan Program). As expected, the aryl fluorine atoms are not as highly charged as the benzylic fluorines (Figure 6a and b). On the other hand, a contour slice (Figure 6c) shows that the electron density from the aryl fluorine lone pairs points directly at the benzylic σ^*(C–F). As shown in Figure 6d, a bond critical point (BCP)

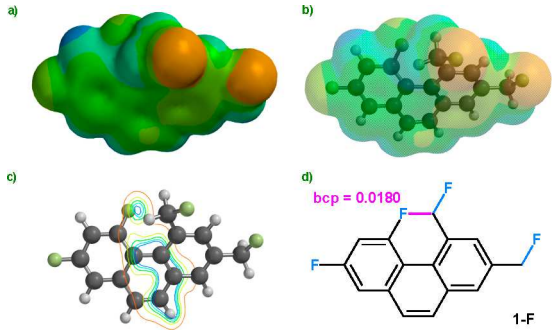

Figure 6. (a) Electrostatic potential map of **1-F** (M06), where orange is negative and blue is positive. (b) Transparent variant of panel a. (c) Electron density slice bisecting the C–F···C-F interaction. (d) AIM bond-critical point between C and F.

https://doi.org/10.1021/acs.joc.2c01788
J. Org. Chem. 2022, 87, 13406–13410

with an electron density of 0.018 e Å^{-3} between the two C−F groups confirms a weak interaction.

The crystal structures shown in Figure 7 provide a wealth of information about the interaction of the aryl C−F bond with

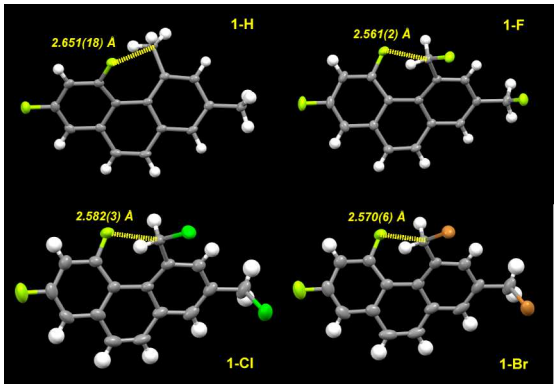

Figure 7. Crystal structures of **1-H**, **1-F**, **1-Cl**, and **1-Br**. Diplacement ellipsoids are given at the 50% probability level.

various electrophilic carbon centers. The control **1-H**, containing a simple methyl group, provides the baseline in which the stabilizing n → σ* and dipolar (C−F···H−C) interactions are expected to be small.[7,22] On the other hand, **1-F** reveals a different scenario; aligned as if it were poised to receive an S_N2 attack,[10,23] the electrophilic fluorine-substituted carbon atom yields a much more substantial interaction (from 2.6513(18) to 2.561(2) Å). Interestingly, this distance is close to that observed theoretically for the backside ion molecule complex of F− and CH_3F in the gas phase (M06, calcd. 2.53 Å). In difluoride−dichloride **1-Cl**, the C−F···C−Cl distance is elongated (2.578(3) Å). The difluoride−dibromide **1-Br** similarly demonstrates the trend, as the C−F···C-Br distance increases slightly to 2.570(6) Å. In terms of bond angles, they are all splayed, as would be expected for a developing S_N2 array.[24] For example, in **1-F**, the F−C−F bond angle is 164°. Molecules **1-H** through **1-Br** are chiral; in contrast, the diastereotopic protons of the halomethyl group in **1-F** through **1-Br** present as one discrete resonance on the NMR time scale at all accessible temperatures. This observation is consistent with a low barrier to enantiomerization in molecules **1-H** through **1-Br**. For example, the calculated barrier to enantiomerization in **1-F** (M06) is only 5.9 kcal/mol.

Although the Ar−F···C−X interaction is static in regard to S_N2 reactivity, the situation could be different in the case of S_N1 conditions. Figure 8 shows two examples of differential reaction chemistry. Under S_N2 conditions (TBAF and MeCN), **1-Br** displays preferential reactivity at the distal bromomethyl group (extrapolated to 0% conversion). In contrast, under S_N1 conditions (LiOAc and AcOH at 100 °C) the preferential reaction occurs at the probe bromomethyl group, implying participation by the C−F bond. A DFT calculation of the intermediate carbocation (M06, "**1-cation**") reveals a benzyl cation slightly stabilized by lone pair density from fluorine (C−F distance calcd. 2.6 Å), (Figure 9).[25] Strain relief[26] and the anchimeric assistance from fluorine[27] could play a role in the rate acceleration; the two factors could be intricately linked.

Finally, we used a minimalist model system (a linear CH_3F−CH_3F array constrained to a F···C distance of 2.48 Å) to examine molecular orbital interactions (M06) without interference from other parts of the molecule. The four-

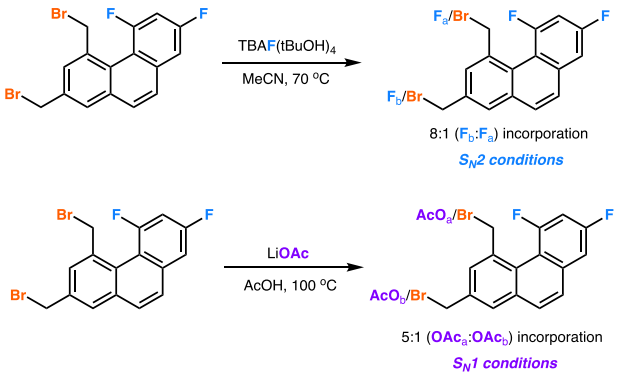

Figure 8. Reaction chemistry.

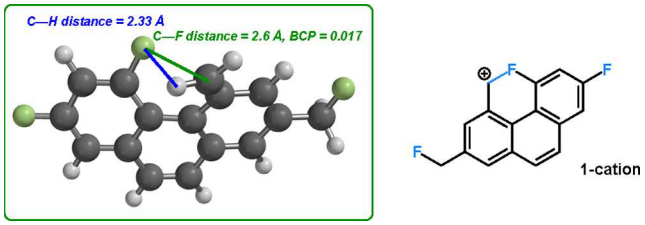

Figure 9. Calculated structure of **1-cation**.

centered orbital shown in Figure 10 shows the key interaction involving lone pairs on F and C−F single bonds.

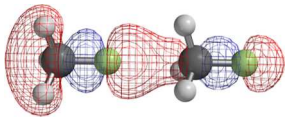

Figure 10. Key orbital interaction of the CH_3F···CH_3F array.

In the near future, we intend to expand the concept of "frozen" nucleophilicity to complementary systems.

■ ASSOCIATED CONTENT

Supporting Information

The Supporting Information is available free of charge at https://pubs.acs.org/doi/10.1021/acs.joc.2c01788.

Experimental procedures, spectra, and computational data (PDF)

Accession Codes

CCDC 2192623−2192626 contain the supplementary crystallographic data for this paper. These data can be obtained free of charge via www.ccdc.cam.ac.uk/data_request/cif, or by emailing data_request@ccdc.cam.ac.uk, or by contacting The Cambridge Crystallographic Data Centre, 12 Union Road, Cambridge CB2 1EZ, UK; fax: +44 1223 336033.

■ AUTHOR INFORMATION

Corresponding Author

Thomas Lectka − *Department of Chemistry, Johns Hopkins University, Baltimore, Maryland 21218, United States;* orcid.org/0000-0003-3088-6714; Email: lectka@jhu.edu

https://doi.org/10.1021/acs.joc.2c01788
J. Org. Chem. 2022, 87, 13406−13410

Authors

Stefan Andrew Harry − *Department of Chemistry, Johns Hopkins University, Baltimore, Maryland 21218, United States;* orcid.org/0000-0002-5479-4008

Nathaniel G. Garrison − *Department of Chemistry, Johns Hopkins University, Baltimore, Maryland 21218, United States;* orcid.org/0000-0001-8715-2346

Andrea Zhu − *Department of Chemistry, Johns Hopkins University, Baltimore, Maryland 21218, United States*

Michael Richard Xiang − *Department of Chemistry, Johns Hopkins University, Baltimore, Maryland 21218, United States*

Maxime A. Siegler − *Department of Chemistry, Johns Hopkins University, Baltimore, Maryland 21218, United States;* orcid.org/0000-0003-4165-7810

Complete contact information is available at: https://pubs.acs.org/10.1021/acs.joc.2c01788

Notes

The authors declare no competing financial interest.

■ ACKNOWLEDGMENTS

T.L. thanks the National Science Foundation (NSF) (Grant CHE 2102116) for financial support. Mass spectral data were obtained at University of Delaware's mass spectrometry centers.

■ REFERENCES

(1) (a) Park, B. K.; Kitteringham, N. R.; O'Neill, P. M. Metabolism of fluorine-containing drugs. *Annual Review of Pharmacology and Toxicology* **2001**, *41*, 443−470. (b) Meanwell, N. A. Fluorine and Fluorinated Motifs in the Design and Application of Bioisosteres for Drug Design. *J. Med. Chem.* **2018**, *61*, 5822−5880. (c) Hagmann, W. K. The Many Roles for Fluorine in Medicinal Chemistry. *J. Med. Chem.* **2008**, *51*, 4359−4369.

(2) (a) Sun, L.; Song, K.; Hase, W. L. A S_N2 Reaction That Avoids Its Deep Potential Energy Minimum. *Science* **2002**, *296*, 875−878. (b) Ensing, B.; Klein, M. L. Perspective on the reactions between F− and CH_3CH_2F: The free energy landscape of the E2 and S_N2 reaction channels. *Proc. Nat. Acad. Sci.* **2005**, *102*, 6755−6759. (c) Mitchell, D. J.; Schlegel, H. B.; Shaik, S. S.; Wolfe, S. Relationships between geometries and energies of identity S_N2 transition states: The dominant role of the distortion energy and its origin. *S. Can. J. Chem.* **1985**, *63*, 1642−1648.

(3) For a recent review on the mechanism of the S_N2 reaction, see: Hamlin, T. A.; Swart, M.; Bickelhaupt, F. M. Nucleophilic Substitution (S_N2): Dependence on Nucleophile, Leaving Group, Central Atom, Substituents, and Solvent. *ChemPhysChem* **2018**, *19*, 1315−1330.

(4) Harder, S.; Streitwieser, A.; Petty, J. T.; von Schleyer, P. Ion Pair S_N2 Reactions. Theoretical Study of Inversion and Retention Mechanisms. *J. Am. Chem. Soc.* **1995**, *117*, 3253−3259.

(5) Mani, D.; Arunan, E. The X−C···Y (X = O/F, Y = O/S/F/Cl/Br/N/P) 'carbon bond' and hydrophobic interactions. *Phys. Chem. Chem. Phys.* **2013**, *15* (34), 14377−14383.

(6) (a) Bundhun, A.; Ramasami, P.; Murray, J. S.; Politzer, P. (2013). Trends in σ-hole strengths and interactions of F3MX molecules (M = C, Si, Ge and X = F, Cl, Br, I). *J. Mol. Model.* **2013**, *19* (7), 2739−2746. (b) Bauzá, A.; Mooibroek, T. J.; Frontera, A. Tetrel-Bonding Interaction: Rediscovered Supramolecular Force? *Angew. Chem., Int. Ed.* **2013**, *52*, 12317−12321.

(7) Daolio, A.; Scilabra, P.; Terraneo, G.; Resnati, G. C(sp^3) atoms as tetrel bond donors: A crystallographic survey. *Coord. Chem. Rev.* **2020**, *413*, 213265.

(8) Stanford, M. W.; Knight, F. R.; Athukorala Arachchige, K. S.; Sanz Camacho, P.; Ashbrook, S. E.; Bühl, M.; Slawin, A. M. Z.; Woollins, J. D. Probing interactions through space using spin−spin coupling. *Dalton Trans* **2014**, *43* (17), 6548−6560.

(9) Scheiner, S. Origins and properties of the tetrel bond. *Phys. Chem. Chem. Phys.* **2021**, *23* (10), 5702−5717.

(10) Grabowski, S. J. Tetrel bond−σ-hole bond as a preliminary stage of the S_N2 reaction. *Phys. Chem. Chem. Phys.* **2014**, *16* (5), 1824−1834.

(11) (a) Cosmo, R.; Hambley, T. W.; Sternhell, S. Skeletal deformation in 4,5-disubstituted 9,10-dihydrophenanthrenes and 4,5-disubstituted phenanthrenes. *J. Org. Chem.* **1987**, *52*, 3119−3123. (b) Cosmo, R.; Sternhell, S. Steric Effects. Inversion of 4,5-Disubstituted 9,10-Dihydrophenanthrenes. *Aus. J. Chem.* **1987**, *40*, 35−47. (c) Newman, M. S.; Wheatley, W. B. Optical Activity of the 4,5-Phenanthrene Type: 4-(l-Methylbenzo[c]phenanthryl)-acetic Acid and 1-Methylbenzo[c]phenanthrene. *J. Am. Chem. Soc.* **1948**, *70*, 1913−1916.

(12) We recently used this scaffold to examine the close interaction of a C−F bond with an amide carbonyl group: Harry, S. A.; Kazim, M.; Nguyen, P. M.; Zhu, A.; Xiang, M. R.; Catazaro, J.; Siegler, M.; Lectka, T. The Close Interaction of a C-F Bond with an Amide Carbonyl: Crystallographic and Spectroscopic Characterization. *Angew. Chem., Int. Ed.* **2022**, *61*, No. e202207966.

(13) Hilgraf, R.; Pfaltz, A. Chiral Bis (N-sulfonylamino) phosphine- and TADDOL-Phosphite-Oxazoline Ligands: Synthesis and Application in Asymmetric Catalysis. *Adv. Synth. Catal.* **2005**, *347*, 61−77.

(14) Mallory, F. B.; Mallory, C. W. Photocyclization of Stilbenes and Related Molecules. In *Organic Reactions*; John Wiley & Sons, Inc., 2005.

(15) Kim, D. W.; Jeong, H.-J.; Lim, S. T.; Sohn, M.-H. Tetrabutylammonium Tetra (tert-Butyl Alcohol)-Coordinated Fluoride as a Facile Fluoride Source. *Angew. Chem., Int. Ed.* **2008**, *47*, 8404−8406.

(16) Jaszuński, M.; Świder, P.; Sauer, S. P. A. Through-space spin−spin coupling constants involving fluorine: benchmarking DFT functionals. *Mol. Phys.* **2019**, *117*, 1469−1480.

(17) (a) Contreras, R. H.; Giribet, C. G.; Natiello, M. A.; Pérez, J.; Rae, I. D.; Weigold, J. A. Experimental and Theoretical-Study of Carbon-Fluorine Couplings in the NMR-Spectra of 2-Fluoroaryl Ketones. *Aust. J. Chem.* **1985**, *38*, 1779−1784. (b) Shimoni, L.; Carrell, H. L.; Glusker, J. P.; Coombs, M. M. Intermolecular effects in crystals of 11-(trifluoromethyl)-15,16-dihydrocyclopenta[a]-phenanthren-17-one. *J. Am. Chem. Soc.* **1994**, *116*, 8162−8168. (c) Hsee, L. C.; Sardella, D. J. Through-space $^{13}C-^{19}F$ couplings in highly-crowded systems: Radial dependence and electronic effects. *Magn. Reson. Chem.* **1990**, *28*, 688−692.

(18) Calculations were performed using the following program: *Spartan'18*; Wavefunction, Inc.: Irvine, CA, 2018.

(19) Gillis, E. P.; Eastman, K. J.; Hill, M. D.; Donnelly, D. J.; Meanwell, N. A. Applications of fluorine in medicinal chemistry. *J. Med. Chem.* **2015**, *58* (21), 8315−8359.

(20) Levandowski, B. J.; Raines, R. T.; Houk, K. N. Hyperconjugative $\pi \rightarrow \sigma^*$ CF Interactions Stabilize the Enol Form of Perfluorinated Cyclic Keto−Enol Systems. *J. Org. Chem.* **2019**, *84* (10), 6432−6436.

(21) Bryce, D. L.; Wasylishen, R. E. Ab initio characterization of through-space indirect nuclear spin-spin coupling tensors for fluorine-X (X = F, C, H) spin pairs. *J. Mol. Struct.* **2002**, *602*−*603*, 463−472.

(22) Shimoni, L.; Glusker, J. P. The geometry of intermolecular interactions in some crystalline fluorine-containing organic compounds. *Struct. Chem.* **1994**, *5*, 383−397.

(23) Mondal, R.; Agbaria, M.; Nairoukh, Z. Fluorinated Rings: Conformation and Application. *Chem. -Eur. J.* **2021**, *27*, 7193−7213.

(24) Fox, J. M.; Dmitrenko, O.; Liao, L. A.; Bach, R. D. Computational Studies of Nucleophilic Substitution at Carbonyl Carbon: the S_N2 Mechanism versus the Tetrahedral Intermediate in Organic Synthesis. *J. Org. Chem.* **2004**, *69*, 7317−7328.

(25) Fuchibe, K.; Mayumi, Y.; Zhao, N.; Watanabe, S.; Yokota, M.; Ichikawa, J. Domino Synthesis of Fluorine-Substituted Polycyclic

Aromatic Hydrocarbons: 1,1-Difluoroallenes as Synthetic Platforms. *Angew. Chem., Int. Ed.* **2013**, *52*, 7825−7828.
(26) (a) Slutsky, J.; Bingham, R. C.; Schleyer, P. v. R.; Dickason, W. C.; Brown, H. C. Remarkably large solvolytic rate enhancement due to relief of ground state leaving group strain. *J. Am. Chem. Soc.* **1974**, *96*, 1969−1970. (b) Mergelsberg, I.; Rüchardt, C. The solvolysis of 1− and 3-homoadamantyl-p-nitrobenzoates in acetonitrile-water (70:30 by weight). *Tetrahedron Lett.* **1982**, *23*, 1809−1812.
(27) (a) Struble, M. D.; Holl, M. G.; Scerba, M. T.; Siegler, M. A.; Lectka, T. Search for a Symmetrical C−F−C Fluoronium Ion in Solution: Kinetic Isotope Effects, Synthetic Labeling, and Computational, Solvent, and Rate Studies. *J. Am. Chem. Soc.* **2015**, *137*, 11476−11490. (b) Struble, M. D.; Scerba, M. T.; Siegler, M.; Lectka, T. Evidence for a Symmetrical Fluoronium Ion in Solution. *Science* **2013**, *340*, 57−60.

https://doi.org/10.1021/acs.joc.2c01788
J. Org. Chem. 2022, 87, 13406−13410